



RESEARCH PAPER



## Molecular regulation of miR-378 on the development of mouse follicle and the maturation of oocyte *in vivo*

Xiao-Feng Sun<sup>a</sup>, Ya-Peng Li<sup>b</sup>, Bo Pan <sup>c</sup>, Yu-Feng Wang<sup>a</sup>, Julang Li <sup>c</sup>, and Wei Shen<sup>a</sup>

<sup>a</sup>College of Life Sciences, Institute of Reproductive Sciences, Qingdao Agricultural University, Qingdao, China; <sup>b</sup>College of Animal Science and Technology, Qingdao Agricultural University, Qingdao, China; <sup>c</sup>Department of Animal BioSciences, University of Guelph, Guelph, Ontario, Canada

### ABSTRACT

MicroRNAs (miRNAs) are small, endogenous, non-coding RNAs which can bind to completely or partially complementary sequences in the 3'UTR of target mRNAs, therefore degrading the mRNA or repressing translation. We previously reported that miR-378 played a role in estradiol production via suppression of aromatase translation in porcine granulosa cells and could affect oocyte maturation *in vitro* by inhibiting cumulus cell expansion. However, the role of miR-378 on ovary development *in vivo* is unknown. The current study aimed to uncover the molecular mechanism of miR-378 in regulating mouse follicular development via micro-injection of CMV-miR-378 lentivirus into the bursa of mouse ovary. The results showed that CMV-miR-378 lentivirus transduction in the mouse ovaries resulted in reduced ovary size, extended oestrous cycle (6–7 d in miR-378 overexpression group and 4–5 days in GFP control group) due to continuous oestrus, decreased percentage of oocytes *in vitro* maturation rate (IVM 60.8% vs. 89.4% in GFP control), increased apoptosis rate (Bax/Bcl2 in mRNA and protein level), decreased expression of genes associated with gap junction, such as connexin 43 (Cx-43) and connexin (Cx-37) and decreased expression of genes associated with follicular development, such as BMP15 and GDF9. Moreover, the number of pups/litter was consistently lower in the miR-378 group in each batch of the paired breeding. Our data suggest that miR-378 alters gene expression in cumulus cells and indirectly influences oocyte maturation competency, possibly via inhibition of oocyte-cumulus interaction or induction of apoptosis.

### ARTICLE HISTORY

Received 26 April 2018  
Revised 13 August 2018  
Accepted 28 August 2018

### KEYWORDS

Mir-378; follicular development; oocyte maturation; mouse

### Introduction

MicroRNAs (miRNAs), a class of endogenous small RNA molecules act as one of the important posttranscriptional regulators to exert their functions primarily by binding to completely or partially complementary sequences of the 3' untranslated region (UTR) of the target mRNAs thereby inhibiting the translation of target mRNAs or inducing their degradation [1,2]. Moreover, it has been reported that miRNAs can bind to the 5' UTR of the target mRNAs [3]. These small RNAs were first discovered to control time-dependent developmental events in *Caenorhabditis elegans* [4,5] and had been found evolutionarily conserved among various eukaryotic species [6–8]. These non-coding miRNAs are involved in diverse physiological processes, several developmental and cellular processes including the cell cycle, cell

division, cell differentiation, cell proliferation, and tumorigenesis [9–12].

Mammalian ovary is the most dynamic organ in the adult female with continual activation and development of its follicles and corpora lutea (CL). One of the main functions of the ovary is to produce functional oocyte to allow transmitting genetic information to subsequent generations. MicroRNAs profiling studies in ovary organ of various species confirmed the expression of miRNAs in mammalian ovary [13]. Different miRNAs KO animal models have been confirmed the important roles of miRNAs in ovarian function [14].

Previous studies investigated the roles of miR-378 on mammal reproductive system *in vitro*. Schauer et al. reported that miR-378 expression in equine ovary was dependent on stage of follicular development and its level was inversely correlated to the levels of estradiol in the follicular

fluid in vivo [15]. In addition, miR-378 was revealed to be one of the sixteen miRNAs that were enriched in the exosome of follicular fluid, again suggesting its potential important role in ovarian follicle fluid [16]. Ma et al. reported the inversed expression between miR-378 and the interferon gamma receptor 1 (IFNGR1) gene, which played a role in luteal cell apoptosis and was predicted to be a target of miR-378 during corpus luteum development, suggesting a potential role of miR-378 in suppressing luteal cell apoptosis through the IFNGR1 gene [17].

We have also previously demonstrated that miR-378 is expressed in porcine granulosa cells. And its expression negatively regulates the aromatase protein expression and thus the production of estradiol. Via site-directed mutagenesis and reporter analysis, our study also revealed that miR-378 targeted to the 3'-UTR of aromatase mRNA [18]. Our subsequent study found that miR-378 was also expressed in cumulus cells of cumulus-oocyte complex (COC) at both germinal vesicle (GV) and MII stages. The expression was stage-dependent, with significantly lower expression level in cumulus cells surrounding MII stage oocytes compared with those surrounding the GV stage oocytes. Over-expression of miR-378 impaired the expansion of porcine cumulus cells and inhibited the maturation of oocytes by targeting aromatase mRNA, whose expression affected the production of estradiol [19]. However, in vitro experiment can not always simulate the complicated signal network and complex hormonal regulation. The current study thus aimed to investigate the molecular mechanism of miR-378 in regulating ovary development in vivo by ovarian intrabursal injection, which had been recognized as an effective method for gene transfer [20,21].

## Materials and methods

### Reagents

Inhibitors of miR-378-3p and miR-378-5p, the chemically modified antisense oligonucleotides for miR-378 mature sequences (stem-loop sequence and the mature sequences of miR-378 shown in Figure. S1A), were purchased from Ribobio

company (Guangzhou, China). 50 $\mu$ M solutions of miR-378-3p inhibitor and miR-378-5p inhibitor were prepared by dissolving freeze-dried powder inhibitors into RNase-free water for use.

### Animals

All procedures described in the present study were reviewed and approved by the Ethical Committee of Qingdao Agricultural University (agreement No. 2015-18). 500 CD-1 female virginal mice (Vital River, Beijing, China) of 5 wk were maintained on a 12:12-h light/dark cycle (lights off at 20:00) and were used for assessing reproductive stage of estrous cycle.

### Production of recombinant lentiviral particles

Cloning of the lentiviral gene transfer plasmids for miR-378 overexpression, pL-SIN-Lenti-H1-miR-378-EF1A-EGFP (Lenti-miR-378), and for control plasmid, pL-SIN-Lenti-EF1A-EGFP (Lenti-GFP), as well as production of recombinant lentiviral particles, was carried out as described previously [19,22]. The recombinant lentiviral particles were duplicated by 293FT cell line. The cell medium including viral particles was harvested and ultracentrifuged at 16,500 g for 90 min at 4°C to obtain high concentrations of virus. After re-suspended, the virus were diluted at a functional titer of  $4.8 \times 10^6$  TU/ml, divided into aliquots, and stored at -80°C until use.

### Assessing reproductive stage of estrous cycle

Assessing the stage of estrous cycle is based on the proportion of cell types observed in the vaginal secretion according to the description of Caligioni [23]. Briefly, gently insert the tip of a plastic pipet filled with 20  $\mu$ l PBS or saline, about 5 mm into the vagina. Flush the vagina gently three to five times with the same PBS/saline solution. Then collect final flush in the pipet tip and place final flush containing vaginal fluid on a glass slide for detecting vaginal smear cytology under light microscope. In proestrus stage, there is a predominance of nucleated epithelial cells in clusters or individually (Figure. S1B). Estrus is distinctively characterized by cornified squamous

epithelial cells, which occur in clusters, with no visible nucleus, granular cytoplasm and irregular cellular shape (Figure. S1C). In metestrus stage, there is a mix of cell types with a predominance of leukocytes and a few nucleated epithelial and/or cornified squamous epithelial cells (Figure. S1D). Vaginal smear in diestrus stage consists predominantly of leukocytes (Figure. S1E). Two consecutive baseline cycles were recorded and 200 mice at dioestrus stage and with regular 4–5 d' estrous cycle were selected for the following experimental procedure. After ovarian bursa injection of lentivirus or inhibitors, the stages of estrous cycle were continued to be determined daily to estimate the effects of miR-378 on mice estrous cycle.

### Ovary bursa micro injection

After anesthetized, the mice were carried out operation to ovary-subcutaneously micro-inject virus particles and miR-378 inhibitors using a syringe with a glass micro-injection needle of 50µm diameter. The selected mice were randomly divided into 4 groups for injection of miR-378 virus particles (378 group), GFP virus particles (GFP group), miR-378-3p inhibitor plus miR-378-5p inhibitor (inhibitor group) and miR-378 virus particles plus inhibitors (378 + inhibitor group). After the back skin and muscles of mouse were incised, the bilateral ovaries were carefully pull out and the membrane of ovaries was pull up by tweezers under microscope to keep a space between membrane and ovary thus avoid ovary injury during micro-injection. The dosage of lentivirus particles for one ovary was 2µl, and the dosage had been confirmed to effectively transfect the ovarian cells. We use 25pM miR-378-3p inhibitor plus 25pM miR-378-5p inhibitor for one ovary to inhibit the expression of mature miR-378.

### Calculation of index of ovary/body weight

On the 10th day after micro-injection, the injected mice were weighted and euthanased. Then the ovaries were extirpated and removed the redundant tissue. The ovaries were weighted and recorded. Calculate the index of ovary/body weight using the weight of ovary divided by body weight.

### Quantitative real-time PCR

RNA extraction kit (Aidlab, Beijing, China) was used to isolate total RNAs from the treated and control ovaries according to the manufacturer's instructions. The cDNA was synthesized using the TransScript One-Step kit (TransGen Biotech, Beijing, China). The synthesized cDNA was used as templates to perform quantitative real-time PCR (qRT-PCR) with a Roche real time PCR instrument (Roche LC480, Germany) following the manufacturer's recommendations. Amplification was performed in 10 µl reaction volumes, including 5 µl of SYBR green master mix, 3.6 µl of nuclease-free water, 1 µl of cDNA and 0.4 µl primers (10 µM). PCR reactions were initiated at 95°C for 10 min, followed by denaturing at 95°C for 10 sec, annealing at 60°C for 30 sec and 72°C for 10 sec. After 40 cycles, there was a cooling step at 4°C [24]. Housekeeping gene *GAPDH* was used to normalize the gene expression level. The relative expression for each gene was calculated using  $2^{-(\text{target gene CT value} - \text{reference gene CT value})}$ . Primers sequences and expected product sizes were listed in Table 1.

### Western blotting

Protein lysates isolated from the treated and control ovaries with RIPA lysis solution were used for western blotting analysis according to standard methods [25,26]. Briefly, after 10% SDS-PAGE gel electrophoresis, proteins were transferred onto PVDF membranes. Following blocking with 5% BSA in Tris-buffered saline (TBS) pH 7.4, the membranes were incubated with the first antibody ( $\beta$ -ACTIN, Abcam, ab8226, USA; Aromatase, Abcam, ab18995, USA; Bcl-2, Beyotime, AB112, China; Bax, Cell signaling, 2772, USA; Cx43, Abcam, ab47368, USA; Cx37, Sangon, D152971, China; GFP, Abcam, ab290, USA;), at a dilution of 1:1000 overnight at 4°C. Then the membranes were incubated at 37°C for 2 h with the corresponding second antibody (Goat anti mouse IgG (H + L), Beyotime, A0216, Nantong, China; Goat anti rabbit IgG (H + L), Beyotime, A0208, Nantong, China) conjugated with HRP at a dilution of 1:2000 in TBST after washing three times

**Table 1.** Primers used for quantitative-PCR amplification.

Genes	Sequences of primers	Production(bp)	Genbank
<i>GAPDH</i>	F:5' - GTGTTCTACCCCAATGTG -3' R:5' - GTCATTGAGAGCAATGCCAG -3'	299	XM_017321385
<i>Bax</i>	F:5' - AGACAGGGCCTTTTGTCTAC -3' R:5' - AATTCGCCGGAGACTCG -3'	137	NM_007527
<i>Bcl-2</i>	F:5' - GCTACCGTGTGACTTCGC -3' R:5' - CCCACCGAACTCAAAGAAGG -3'	147	NM_177410
<i>BMP-15</i>	F:5' - TGGGGAGTGGTGCTTTTATG -3' R:5' - GGGCAATGTAGGGTCGTCAG -3'	93	NM_009757
<i>GDF-9</i>	F:5' - GTCACCTCTACAATACCGTCCG -3' R:5' - CACCCGGTCCAGGTTAAACA -3'	119	NM_008110
<i>c-Kit</i>	F:5' - GCCTGACGTGCATTGATCC -3' R:5' - AGTGGCCTCGGCTTTTCC -3'	110	NM_001122733
<i>Cx-43</i>	F:5' - ACAAGTCCAAGCCTACTCCA -3' R:5' - CCGGGTTGTTGAGTGTACAG -3'	145	NM_010288
<i>Cx-37</i>	F:5' - TCCCACATCCGATACTGGGT -3' R:5' - CCCGCCGAGACAGGTAGAT -3'	91	NM_008120

in TBST. The band intensity was quantified using  $\beta$ -Actin as internal control and measured with Alpha view software.

### HE staining

After collected, ovaries from different groups were fixed in 4% paraformaldehyde overnight. Then they were washed by running water, dehydrated by gradient alcohols, and imbedded in paraffin. Serial histological sections of 5  $\mu$ m were obtained and heated at 60°C for 2 hrs. Xylene was used to remove paraffin, gradient alcohols were used to rehydrate the tissues. After the nucleus were stained in hematoxylin for 2 min, the slides were washed by running water for 2 min. Acid alcohol and ammonia solution were then used to differentiate the color and to change the stain from purple to blue respectively. After that, the slides were washed by running water for 5 min and rinsed in 80% alcohol. Cytoplasm were stained in eosin for 15 sec. Vectashield (H-1000; Vector, Shanghai, China) was used to seal the covers and optical microscope was used to take photographs.

### Immunofluorescence

Immunofluorescence was performed to localize the protein expression of Cx43 on the ovary sections of different groups. After fixed in 4% paraformaldehyde (PFA, Beyotime, Nantong, China) overnight, the slides were blocked in ADB solution

(goat serum 0.1 ml, BSA 0.03 g, Triton-X-100 0.5  $\mu$ l, dissolved in 10 ml TBS) for 30 min at 37°C. Then they were incubated with first antibody (Cx43, Abcam, ab47368, USA; 1:100) at 4°C overnight. The next day, the slides were rinsed in PBS containing 1% BSA three times for 15min each and then incubated with Cy3-labeled goat anti-IgG (Beyotime, A0516, 1:100, Nantong, China) at a dilution of 1:150 at 37°C for 1.5 h, followed by incubation with 1  $\mu$ g/ml Hoechst33342 (Sigma, B2261, USA) for 5 min at room temperature. Slides prepared from the same sample and stained with the same procedure but without secondary antibodies served as negative control of immunofluorescence staining. Vectashield (Vector, H-1000) was used to seal the covers just as the procedure of HE staining. Fluorescence intensity was analyzed using LAS-AF-Lite software.

### IVM and spindle assembling analysis

The IVM and spindle assembling were described previously [26]. Briefly, ovaries of mice with different treatments were collected. Antral follicle oocytes were released by puncturing the ovaries and oocytes at GV stage were collected. After washed three times, the oocytes were cultured in the maturation medium ( $\alpha$ -MEM, 10% FCS, 1% penicillin-streptomycin, 1% sodium pyruvate, 100 mIU/ml FSH, 1 ng/ml EGF) for 16–18 h. Oocyte maturation status was scored as germinal vesicle (GV) when the germinal vesicle was

present, as germinal vesicle breakdown (GVBD) when the germinal vesicle had broken down, and as metaphase II (MII) when the Wrst polar body had been extruded. The percentage of IVM was calculated by the number of GVBD and MII oocytes/total oocytes. After 16–18 h IVM, the oocytes were incubated in 4% paraformaldehyde for 30 min at room temperature (RT). The zona pellucida (ZP) was then removed with acidic M2 (Millipor MR-015-D, USA, adjust to pH = 2.5 before use) and incubated with  $\alpha$ -tubulin antibody (Sigma F2168, USA) in cassette for 2 h at RT and stained with propidium iodide (PI) for 15 min. Finally, the spindle assembling of the oocytes was observed with a laser scanning confocal microscope (Leica TCS SP5, Germany).

### Statistical analysis

Data are represented as mean  $\pm$  SD. Differences between the control and treatment groups were statistically determined by one-way analysis of variance (ANOVA) followed by Dunnett's test for multiple comparisons and Student's t-test was used when two groups were compared using Graph-Pad Prism analysis software (Graph-Pad Software, San Diego, CA). \*P < 0.05; \*\*P < 0.01; \*\*\*P < 0.001.

## Results

### Assessment the viability and specificity of miR-378

In order to achieve the overexpression of miR-378 in mouse ovary, we injected miR-378-GFP recombinant lentivirus into the bursa of ovaries. On the 10th day after injection, the mice were euthanized. As soon as the ovaries were extirpated, they were directly photographed under fluorescent microscope, from which, obvious green fluorescence can be observed in the ovaries injected with GFP and miR-378 recombinant virus particles and no GFP signals were detected in non-injected ovaries (Figure. S1F-H). The results of western blotting also confirmed GFP expression at protein level (Figure. S1I). qRT-PCR was then performed to further validate the expression of miR-378. From Figure 1(a), we can see that after miR-378 injection, both miR-378-3p and miR-378-5p increased.

Especially for miR-378-5p, whose expression significantly increased more than 9 times in miR-378 overexpression ovaries than that in control group (GFP recombinant virus particles injected ovaries) (Figure 1(a)). To exclude the toxic effects of miR-378 and to verify that all phenotypes observed were specifically caused by miR-378, inhibitors for miR-378-3p and miR-378-5p were utilized. And the results of qRT-PCR showed that miR-378 inhibitors inhibited the expression of mature miR-378-3p and miR-378-5p, and miR-378 can rescue the decreased expression caused by inhibitor (miR-378+ In group in Figure 1(a)).

### MicroRNA-378 disrupted the mouse estrous cycle

Figure 1(b) showed that miR-378 overexpression disturbed the regular estrous cycle, and made the estrous cycle 4 d longer on average than normal because of their continuous oestrus. At the same time, the expression of aromatase, a target of miR-378, decreased as revealed via western blotting after miR-378 overexpression. As expected, inhibitors of miR-378 increased the expression of aromatase gene at protein level. And the expression level of aromatase protein in the ovaries of miR-378+ In group was between miR-378 group and Inhibitor group (Figure 1(c)).

### MicroRNA-378 decreased the index of ovary body weight

To assess the effects of miR-378 on ovary development, index of ovary body weight was introduced by calculating the value of ovary weight/body weight. Representative images of ovaries morphology showed that miR-378 overexpression reduced the size of ovaries (Figure 2(a)), as well as the index of ovary body weight, with an approximate decrease of 36 percent (Figure 2(b)). To clarify the reasons resulting in these changes, we detected the expression of apoptosis-related genes Bax and Bcl-2. The results showed that miR-378 significantly promoted the ratio of Bax/Bcl-2 both at mRNA level (Figure 2(c)) and at protein level (Figure 2(d)). While, the ovaries injected with inhibitors had a significant decrease in the ratio of Bax/Bcl-2 at protein level (Figure 2(d)). And miR-378 could rescue the

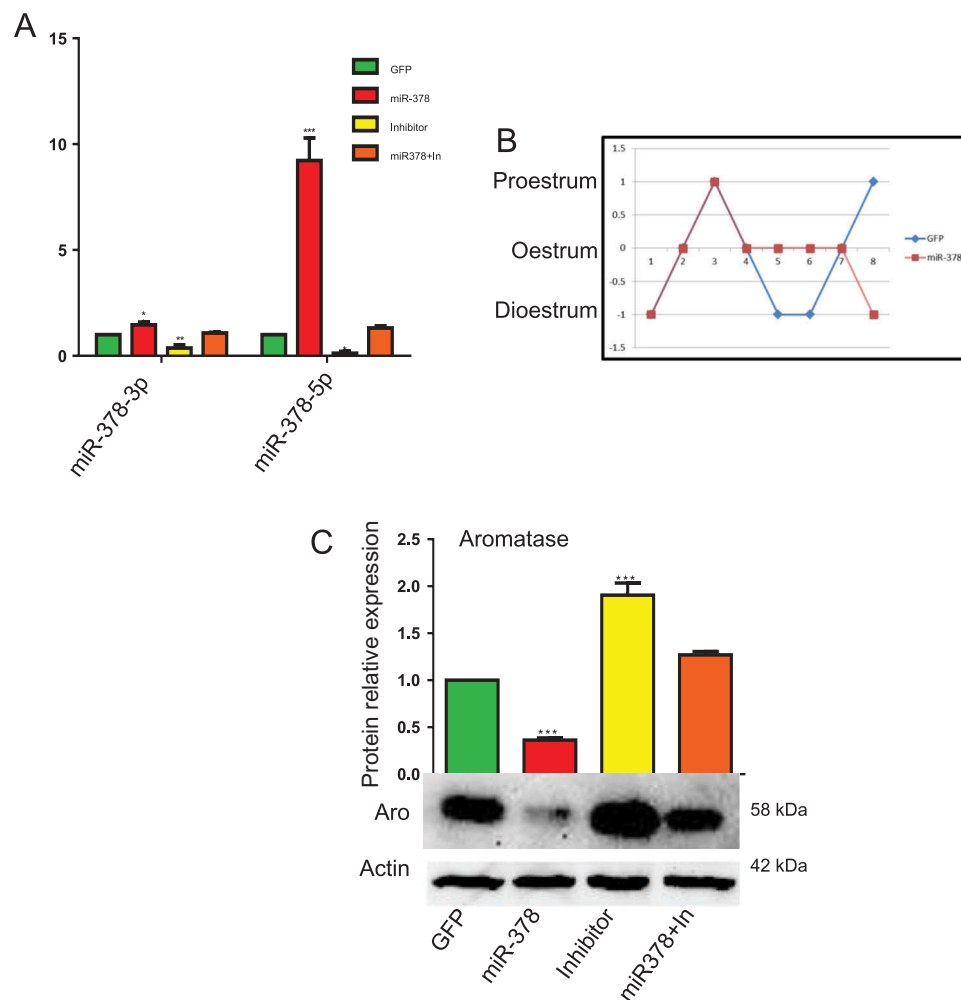


**Figure 1.** MicroRNA-378 disrupted the mouse estrous cycle. (a) The expression of miR-378-3p and miR-378-5p determined by quantitative PCR. (b) Estrous cycle after ovary-subcutaneous injection. The mice were injected at dioestrus. They were at the same stage of estrous cycle over the next 2–3 d, then the estrus of mice with miR-378 overexpression lasted much longer than that of control group (4 d in miR-378 group and 2 d in GFP group). (c) Aromatase expression after microinjection of GFP control, miR-378, Inhibitors and miR-378+ inhibitors determined by western blotting. Data are Mean  $\pm$  SD of at least 3 independent experiments; \*P < 0.05; \*\*P < 0.01; \*\*\*P < 0.001.

decrease induced by miR-378-3p and miR-378-5p inhibitors (Figure 2(d)).

### MicroRNA-378 influenced follicular development

The results of HE staining showed that miR-378 increased the total number of follicles (Figure 3(a-d)) and the dominant follicles were those with diameter

< 150 $\mu$ m after miR-378 overexpression. Overexpression of miR-378 significantly increased the number of follicles with diameter < 150 $\mu$ m, however, significantly decreased the number of follicles with diameter > 250  $\mu$ m (Figure 3(b-d)), suggesting that miR-378 affected the development of ovarian follicles. Even though miR-378 increased the total number of follicles, most of them were smaller follicles with

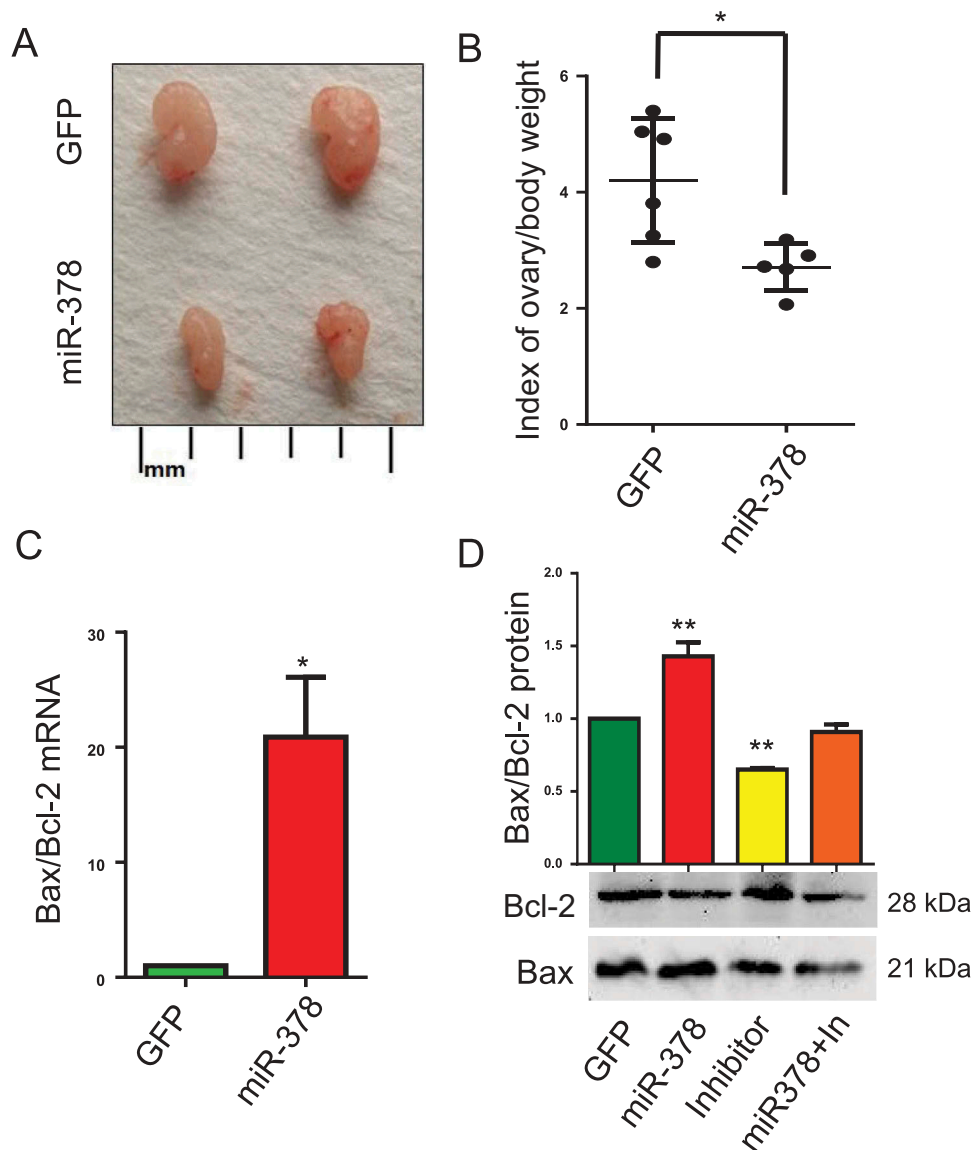


**Figure 2.** Effects of miR-378 on ovary development. (a) Ovarian size and morphology. (b) Index of ovary/body weight. (c) The mRNA ratio of Bax/Bcl-2 determined by quantitative PCR. (d) Bax and Bcl-2 protein expression determined by western blotting. Data are Mean  $\pm$  SD of at least 3 independent experiments; \* $P$  < 0.05; \*\* $P$  < 0.01.

diameter < 150 $\mu$ m. To detect the mRNA expression level of genes related to follicle development, qRT-PCR was performed. The results showed that both BMP-15 and GDF-9, the genes related to follicle development, had significant decreased mRNA expression levels after miR-378 overexpression (Figure 3(e,f)).

#### **MicroRNA-378 decreased oocyte-granulosa interaction**

From the results of HE staining, in miR-378 overexpression ovaries, there was a gap between oocyte and the surrounding granulosa cells

(Figure 3(a)), which showed that miR-378 broke the tight junctions between the granulosa cells and their surrounded oocyte in the follicles. To detect whether the broken tight junctions between the granulosa cells and their surrounded oocyte was associated with the altered relevant gene expression, qRT-PCR and western blotting were performed to quantify the expression level of genes related to oocyte-granulosa interaction such as c-Kit, Cx43 and Cx37. As expected, all of these genes had a significant decreased mRNA expression (Figure 4(a-c)) and a significant decreased protein expression (Figure 4(d,e))

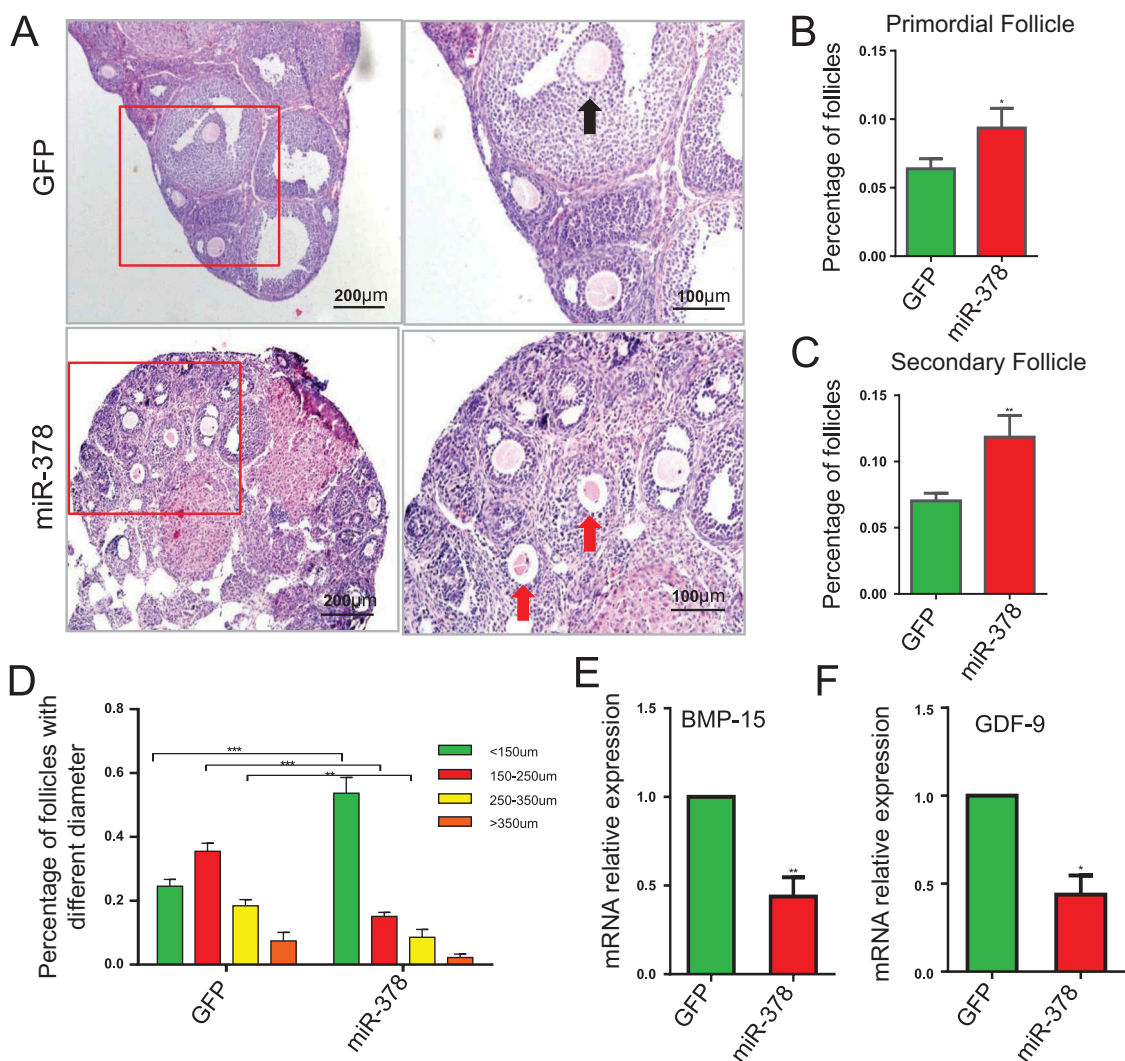


**Figure 3.** Influence of miR-378 on follicle development. (a) Morphological and histochemical analysis by HE staining. (b-d) Percentages of primordial follicles, secondary follicles and antral follicles with different diameter were counted after HE staining. (e, f) The mRNA expression of BMP-15 and GDF-9 determined by quantitative PCR. Data are Mean  $\pm$  SD of at least 3 independent experiments; \*P < 0.05; \*\*P < 0.01; \*\*\*P < 0.001.

after miR-378 ovarian injection. Furthermore, the inhibitors of miR-378-3p and miR-378-5p significantly increased the protein expression of Cx43 and Cx37 (Figure 4(d,e)). Immunohistochemical analysis for Cx43 had the consistent expression results with the western blotting (Figure 5).

#### MicroRNA-378 reduced oocyte maturation rate

Considering the important roles of oocyte-granulosa interaction on oocyte survival and development, we deduced that the broken tight junctions between the granulosa cells and their surrounded oocyte might affect the maturation of oocytes via

blocking the signaling communication and the exchanges of trophic factor. As expected, the percentage of IVM significantly decreased from 89.44% to 60.78% (Figure 6(a,b)) after miR-378 overexpression. And an increased (from 29.53% to 75.57%) abnormal spindle rate was also observed in miR-378 injected ovaries (Figure 6(c,d)). Some treated female mice were maintained at normal condition and were mated with normal male mice. We could see that the average number of pups decreased from 10.13 to 8.857 (Figure 6(e)). Moreover, the number of pups/litter was consistently lower in the miR-378 group in each batch of the paired breeding (Figure 6(f)).



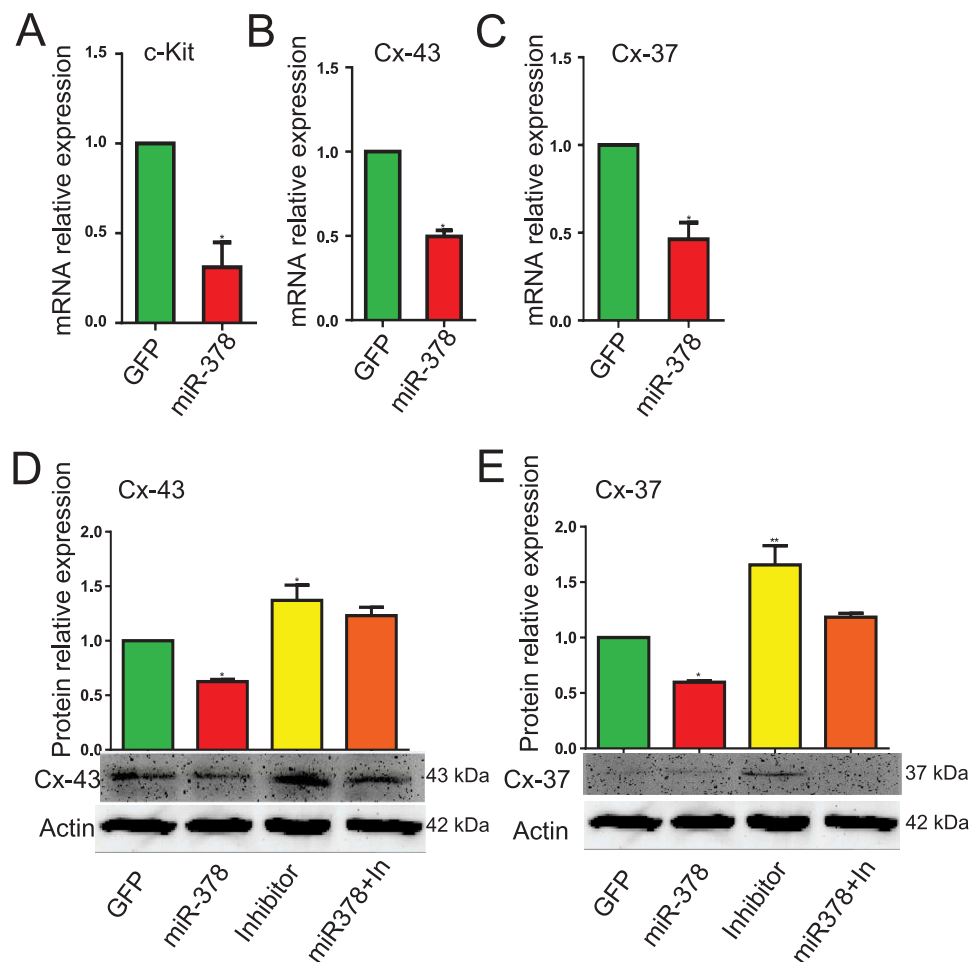


**Figure 4.** MicroRNA-378 decreased the oocyte-granulosa interaction. (a-c) The mRNA expression of c-Kit, Cx-43 and Cx-37 determined by quantitative PCR. (d, e) The protein expression of Cx-43 and Cx-37 determined by western blotting. Data are Mean  $\pm$  SD of at least 3 independent experiments; \*P < 0.05; \*\*P < 0.01.

### MicroRNA-378 affected the F1 offspring

From the results, miR-378 decreased gestational length from 18.88 to 18 d (Figure. S2A). The average body weight at birth of the miR-378 group increased to 2.091g compared to that 1.848g of the GFP control group (Figure. S2B), which maybe resulted from the decreased average number of pups. Interestingly, the ratios of male/female in the pups from GFP control groups were randomly less than 1, equal to 1 and more than 1, while, in the miR-378 groups, the ratios of male/female were all equal or more than 1, none of them was less than 1 (Figure. S2C and D), suggesting that miR-378 overexpression in the ovary resulted in more male than female offspring.

### Discussion

The close association between oocyte and their surrounding somatic cells plays crucial roles for normal oocyte and follicular development [27]. Lying in the outside of the zona pellucida, GCs keep physical, physiological connection with the oocyte through gap junctions and play a very important role in nourishing oocyte through their secretion of growth factors and hormones and regulating oocyte development [28,29]. It is known that gap junctions between GCs and oocytes enable small molecules (such as amino acids, ions and metabolites, etc.) to transfer to the oocyte, which can provide up to 85% of oocyte metabolic needs [29]. Gap junctions are contact-dependent cellular interactions and have

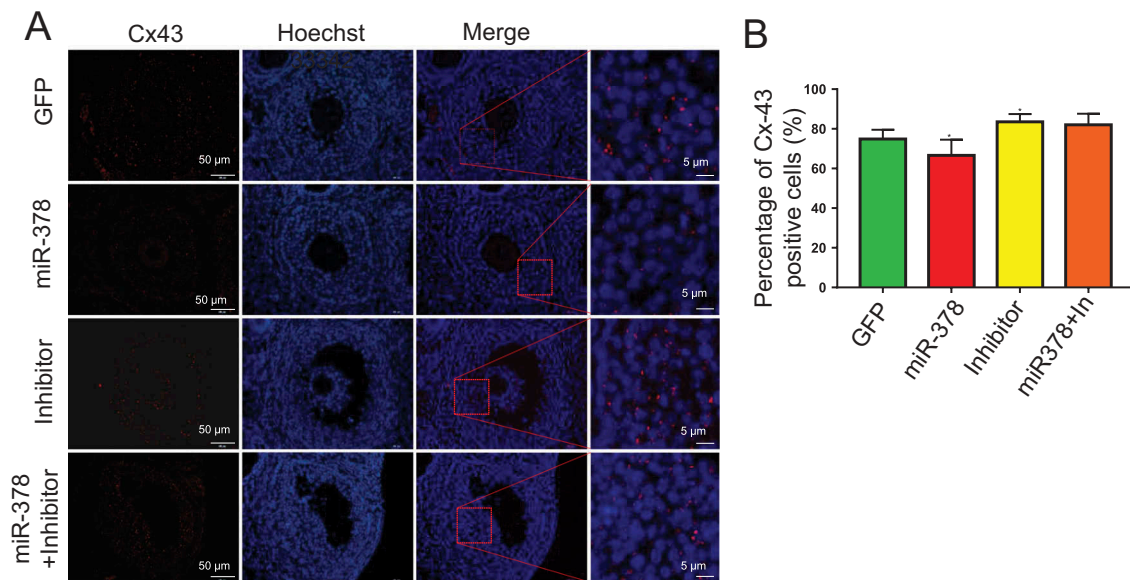


**Figure 5.** The immunofluorescence of Cx-43. (a) Histological sections are stained red with anti-Cx-43 antibody, nuclei are stained blue with Hoechst33342. (b) Percentage of Cx43 positive cells. Data are Mean  $\pm$  SD of at least 3 independent experiments; \* $P < 0.05$ .

a hexameric structure composed of specific gap junctional proteins termed connexins (Cxs) [30]. Among all of the Cxs, Cx37 and Cx43 are most studied and expressed in the oocyte and granulosa cells/cumulus cells respectively. Kit ligand (KL)-c-kit interaction is important in regulation of oogenesis, folliculogenesis, and ovarian steroidogenesis [31]. The authors of this paper also reported that kit ligand suppressed estradiol production and aromatase mRNA expression without affecting progesterone production. And they proved that the suppression of estrogen by granulosa cells was through the interaction of KL on the granulosa cells and c-Kit on the oocyte using anti-c-Kit neutralizing antibody. In our study, we detected a gap between granulosa cells and oocyte by HE staining (Figure 3(a)), which means the interruption of contact-dependent cellular interactions. Meanwhile, the expression of molecules including c-Kit (Figure 4(a)), Cx43 (Figure 4(b, d)) and Cx37 (Figure 4(c, e)) involved in interaction between granulosa cells and oocyte was found decreased after miR-378 injection. Furthermore, decreased aromatase expression (Figure 1(c)) and disturbed estrous cycle by abnormal generative hormones level (Figure 1(b)) were also detected, which we suggested, was caused by the loose of the close connection between granulosa cells and oocyte in the

follicles. The relationship between generative hormones level and connexin (Cx) has been well studied. Estrogens could lead to the increased expression of Cx43 in rat [32–34] and pig [35]. The appearance of the gap and the decrease of the molecules expression level involved in interaction between granulosa cells and oocyte may have blocked the signaling, nutrition, growth factor and steroids transmitting between granulosa cells and oocytes, which induced the apoptosis of granulosa cells and affected the maturation of oocyte and resulted in reduced ovary size (Figure 2(a, b)), as well as oocyte maturation rate (Figure 6(a, b)). Estrogen played roles in promoting the connections between bovine oocyte and granulosa cells, resulting in the complete oocyte growth with bigger OGCs (oocyte–granulosa cell complexes) diameter, bigger oocyte diameter and the acquisition of meiotic competence with higher IVM rate [36]. Moreover, GDF-9 was reported to promote granulosa cell proliferation and differentiation during follicle development and was required for the formation of TZPs in mice, where gap junctions were formed. In our study, miR-378 decreased the expression of GDF-9 (Figure 3(f)), which decreased the granulosa cell proliferation, leading to much more smaller follicles (Figure 3(b–d)) and promoting the formation of the gap between oocyte and granulosa cells.

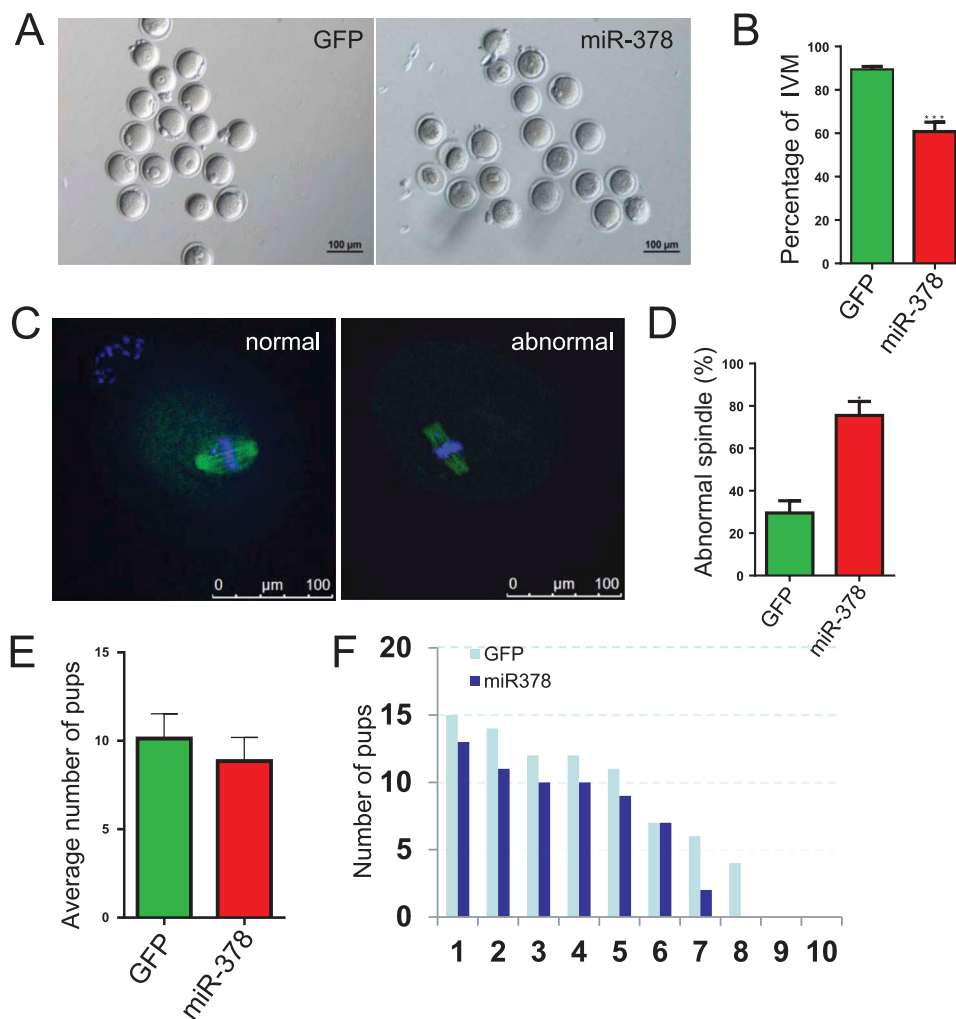


**Figure 6.** MicroRNA-378 reduced the percentage of oocyte maturation. (a) Oocytes after IVM 16–18 h. (b) Percentage of IVM after different treatments. (c) Normal and abnormal spindle assembling of oocytes. (D) The ratio of abnormal spindle assembling of oocytes after different treatments. (e) The treated female mice were maintained at normal condition and were mated with normal male mice. After birth, the average number of pups was counted. (f) The compared number of pups/litter in each batch of the paired breeding. Data are Mean  $\pm$  SD of at least three independent experiments; \* $P < 0.05$ ; \*\* $P < 0.01$ ; \*\*\* $P < 0.001$ .

Inhibitors of miR-378-3p and miR-378-5p had the opposite effects on the expression of aromatase (Figure 1(c)), the ratio of Bax/Bcl-2 (Figure 2(c,d)) and the expression of Cx43 and Cx37 (Figure 4(d, e); Figure 5(a,b)), suggesting the specific effects of miR-378 on ovary.

Furthermore, it was reported that estrogens could increase the ovarian weight [37] and stimulate the proliferation of granulosa cells [38], while the ovarian androgens acting as apoptotic factors could cause deterioration of ovarian follicles by increasing the number of pyknotic granulosa cells and degenerated oocytes and then result in the decreasing ovarian weight [39,40]. An increased androgen to estrogen

ratio was also found in follicular fluid of atretic follicles [41]. All of these reports are in accordance with our results that miR-378 overexpression reduced the translation of aromatase (Figure 1(c)) which decreased the conversion ratio of androgen to estrogen. That's why miR-378 injection induced the index of ovary/body (Figure 2(a,b)). As early as 1975, Louvet et al. showed that androgen promoted the percentage of atretic large follicles instead of small follicles [42]. Several years later, another group got the same results [40,42]. In our study, miR-378 injection led to the decreased number of large follicles (Figure 3(d)), which may be caused by the decreased expression of aromatase, too.

It is interesting to find that miR-378 overexpression in the ovary resulted in more male than female offspring (Figure. S2C and D), the exact mechanism underlying which needs to be further explored. We think it may be due to the disturbed reproductive hormones by miR-378.

## Acknowledgments

This work was supported by Shandong Province Natural Science Foundation of China (ZR2017MC033), National Natural Science Foundation of China (31471346) and the Natural Sciences and Engineering Research Council of Canada (NSERC).



## Disclosure statement

No potential conflict of interest was reported by the authors.

## Funding

This work was supported by the National Natural Science Foundation of China [31471346]; Natural Sciences and Engineering Research Council of Canada; Shandong Province Natural Science Foundation of China [ZR2017MC033].

## ORCID

Bo Pan  <http://orcid.org/0000-0002-0984-2058>  
Julang Li  <http://orcid.org/0000-0002-5794-7727>

## References

- [1] Bartel DP. MicroRNAs: genomics, biogenesis, mechanism, and function. *Cell*. 2004;116:281–297.
- [2] Choi JS, Oh JH, Park HJ, et al. miRNA regulation of cytotoxic effects in mouse Sertoli cells exposed to non-ylphenol. *Reprod Biol Endocrinol: RB&E*. 2011;9:126.
- [3] Orom UA, Nielsen FC, Lund AH. MicroRNA-10a binds the 5'UTR of ribosomal protein mRNAs and enhances their translation. *Mol Cell*. 2008;30:460–471.
- [4] Lee RC, Feinbaum RL, Ambros V. The *C. elegans* heterochronic gene *lin-4* encodes small RNAs with antisense complementarity to *lin-14*. *Cell*. 1993;75:843–854.
- [5] Wightman B, Ha I, Ruvkun G. Posttranscriptional regulation of the heterochronic gene *lin-14* by *lin-4* mediates temporal pattern formation in *C. elegans*. *Cell*. 1993;75:855–862.
- [6] Pasquinelli AE, Reinhart BJ, Slack F, et al. Conservation of the sequence and temporal expression of *let-7* heterochronic regulatory RNA. *Nature*. 2000;408:86–89.

- [7] Lagos-Quintana M, Rauhut R, Lendeckel W, et al. Identification of novel genes coding for small expressed RNAs. *Science*. 2001;294:853–858.
- [8] Lau NC, Lim LP, Weinstein EG, et al. An abundant class of tiny RNAs with probable regulatory roles in *Caenorhabditis elegans*. *Science*. 2001;294:858–862.
- [9] Fire A, Xu S, Montgomery MK, et al. Potent and specific genetic interference by double-stranded RNA in *Caenorhabditis elegans*. *Nature*. 1998;391:806–811.
- [10] Hwang HW, Mendell JT. MicroRNAs in cell proliferation, cell death, and tumorigenesis. *Br J Cancer*. 2007;96(Suppl):R40–R4.
- [11] Williams AH, Liu N, van Rooij E, et al. MicroRNA control of muscle development and disease. *Curr Opin Cell Biol*. 2009;21:461–469.
- [12] Risek Y, Baserga R, Chen L, et al. microRNA, cell cycle, and human breast cancer. *Am J Pathol*. 2010;176:1058–1064.
- [13] Gebremedhn S, Salilew-Wondim D, Ahmad I, et al. MicroRNA expression profile in bovine granulosa cells of preovulatory dominant and subordinate follicles during the late follicular phase of the estrous cycle. *PLoS One*. 2015;10:e0125912.
- [14] Vidigal JA, Ventura A. The biological functions of miRNAs: lessons from in vivo studies. *Trends Cell Biol*. 2015;25:137–147.
- [15] Schauer S, Sontakke S, Watson E, et al. Involvement of miRNAs in equine follicle development. *Reproduction*. 2013;146:273–282.
- [16] da Silveira JC, Veeramachaneni DN, Winger QA, et al. Cell-secreted vesicles in equine ovarian follicular fluid contain miRNAs and proteins: a possible new form of cell communication within the ovarian follicle. *Biol Reprod*. 2012;86:71.
- [17] Ma T, Jiang H, Gao Y, et al. Microarray analysis of differentially expressed microRNAs in non-regressed and regressed bovine corpus luteum tissue; microRNA-378 may suppress luteal cell apoptosis by targeting the interferon gamma receptor 1 gene. *J Appl Genet*. 2011;52:481–486.
- [18] Xu S, Linher-Melville K, Yang BB, et al. MicroRNA378 (miR-378) regulates ovarian estradiol production by targeting aromatase. *Endocrinology*. 2011;152:3941–3951.
- [19] Pan B, Toms D, Shen W, et al. MicroRNA-378 regulates oocyte maturation via the suppression of aromatase in porcine cumulus cells. *Am J Physiol Endocrinol and Metab*. 2015;308:E525–E34.
- [20] Lu X, Guo S, Cheng Y, et al. Stimulation of ovarian follicle growth after AMPK inhibition. *Reproduction*. 2017;153:683–694.
- [21] Flesken-Nikitin A, Choi KC, Eng JP, et al. Induction of carcinogenesis by concurrent inactivation of p53 and Rb1 in the mouse ovarian surface epithelium. *Cancer Res*. 2003;63:3459–3463.
- [22] Xu S, Linher-Melville K, Yang BB, et al. MicroRNA378 (miR-378) regulates ovarian estradiol

- production by targeting aromatase. *Endocrinology*. 2011;152:3941–3951.
- [23] Caligioni CS. Assessing reproductive status/stages in mice. *current protocols in neuroscience*. *Current Protoc in Neurosci*. 2009;48(1):A–41.
- [24] Qin X, Cao M, Lai F, et al. Oxidative stress induced by zearalenone in porcine granulosa cells and its rescue by curcumin in vitro. *PLoS One*. 2015;10:e0127551.
- [25] Zhang P, Chao H, Sun X, et al. Murine folliculogenesis in vitro is stage-specifically regulated by insulin via the Akt signaling pathway. *Histochem Cell Biol*. 2010;134:75–82.
- [26] Chao HH, Zhang XF, Chen B, et al. Bisphenol A exposure modifies methylation of imprinted genes in mouse oocytes via the estrogen receptor signaling pathway. *Histochem Cell Biol*. 2012;137:249–259.
- [27] Buccione R, Schroeder AC, Eppig JJ. Interactions between somatic cells and germ cells throughout mammalian oogenesis. *Biol Reprod*. 1990;43:543–547.
- [28] Jancar N, Kopitar AN, Ihan A, et al. Effect of apoptosis and reactive oxygen species production in human granulosa cells on oocyte fertilization and blastocyst development. *J Assist Reprod Genet*. 2007;24:91–97.
- [29] Luo M, Li L, Xiao C, et al. Heat stress impairs mice granulosa cell function by diminishing steroids production and inducing apoptosis. *Mol Cell Biochem*. 2016;412:81–90.
- [30] Grazul-Bilska AT, Reynolds LP, Redmer DA. Gap junctions in the ovaries. *Biol Reprod*. 1997;57:947–957.
- [31] Miyoshi T, Otsuka F, Nakamura E, et al. Regulatory role of kit ligand-c-kit interaction and oocyte factors in steroidogenesis by rat granulosa cells. *Mol Cell Endocrinol*. 2012;358:18–26.
- [32] Merk FB, Botticelli CR, Albright JT. An intercellular response to estrogen by granulosa cells in the rat ovary; an electron microscope study. *Endocrinology*. 1972;90:992–1007.
- [33] Burghardt RC, Anderson E. Hormonal modulation of gap junctions in rat ovarian follicles. *Cell Tissue Res*. 1981;214:181–193.
- [34] Risek B, Klier FG, Phillips A, et al. Gap junction regulation in the uterus and ovaries of immature rats by estrogen and progesterone. *J Cell Sci*. 1995;108(Pt 3):1017–1032.
- [35] Ciesiolka S, Budna J, Jopek K, et al. Time- and dose-dependent effects of 17 beta-estradiol on short-term, real-time proliferation and gene expression in porcine granulosa cells. *Biomed Res Int*. 2017;2017:9738640.
- [36] Makita M, Miyano T. Steroid hormones promote bovine oocyte growth and connection with granulosa cells. *Theriogenology*. 2014;82:605–612.
- [37] Payne RW, Hellbaum AA. The effect of estrogens on the ovary of the hypophysectomized rat. *Endocrinology*. 1955;57:193–199.
- [38] Bendell JJ, Dorrington J. Estradiol-17 beta stimulates DNA synthesis in rat granulosa cells: action mediated by transforming growth factor-beta. *Endocrinology*. 1991;128:2663–2665.
- [39] Chakraborty T, Mohapatra S, Tobayama M, et al. Hatching enzymes disrupt aberrant gonadal degeneration by the autophagy/apoptosis cell fate decision. *Sci Rep*. 2017;7:3183.
- [40] Azzolin GC, Saiduddin S. Effect of androgens on the ovarian morphology of the hypophysectomized rat. *Proceedings of the Society for Experimental Biology and Medicine Society for Experimental Biology and Medicine*;1983;172:70–73.
- [41] Maxson WS, Haney AF, Schomberg DW. Steroidogenesis in porcine atretic follicles: loss of aromatase activity in isolated granulosa and theca. *Biol Reprod*. 1985;33:495–501.
- [42] Louvet JP, Harman SM, Schrieber JR, et al. Evidence of a role of adrogens in follicular maturation. *Endocrinology*. 1975;97:366–372.